PHILOSOPHICAL TRANSACTIONS OF THE ROYAL SOCIETY A

Phil. Trans. R. Soc. A (2009) **367**, 1195–1212
doi:10.1098/rsta.2008.0278
Published online 16 February 2009

Delay effects in the human sensory system during balancing

By Gabor Stepan*

Department of Applied Mechanics, Budapest University of Technology and Economics, Budapest 1521, Hungary

Mechanical models of human self-balancing often use the Newtonian equations of inverted pendula. While these mathematical models are precise enough on the mechanical side, the ways humans balance themselves are still quite unexplored on the control side. Time delays in the sensory and motoric neural pathways give essential limitations to the stabilization of the human body as a multiple inverted pendulum. The sensory systems supporting each other provide the necessary signals for these control tasks; but the more complicated the system is, the larger delay is introduced. Human ageing as well as our actual physical and mental state affects the time delays in the neural system, and the mechanical structure of the human body also changes in a large range during our lives. The human balancing organ, the labyrinth, and the vision system essentially adapted to these relatively large time delays and parameter regions occurring during balancing. The analytical study of the simplified large-scale time-delayed models of balancing provides a Newtonian insight into the functioning of these organs that may also serve as a basis to support theories and hypotheses on balancing and vision.

Keywords: delay; labyrinth; vision; balancing; postural sway; inverted pendulum

1. Introduction

Balancing ourselves is an essential human property. It has always been an interest of researchers in either medical or physical sciences. Since Newtonian mechanics described and analysed the stable and unstable equilibria of a pendulum by means of differential equations, the inverted pendula have been the obvious subjects for mechanical models of balancing. However, the inverted pendulum is unstable without control actions, and the way we balance this pendulum is a complex and still not fully understood process.

The mechanical models can also be quite complicated if all the mechanical degrees of freedom of a human body are taken into consideration. The labyrinth in the auditory system, the eyes in the visual system and the mechanoreceptors in the touch system all serve as sensory systems for balancing, and the brain uses these inputs in an intricate way to achieve stability. If control actions are considered to happen at the same time instant as when the input signals are detected, the mathematical models are ordinary differential equations—the

*stepan@mm.bme.hu

One contribution of 10 to a Theme Issue ‘Delay effects in brain dynamics’.

identification of the equilibria and the analysis of their stability with the help of the linear variational systems are quite straightforward procedures. This way, simple first approximations can be derived to determine under what conditions balancing is successful.

However, there is a substantial time delay caused by the finite speed of signal propagation in the nervous system. The story of measuring this speed first in 1850 by Helmholtz can be found in Nijhawan (2008), where the most important neural delays are also summarized for the visual system. Recently, Campbell (2007) has given a summary of different kinds of delays occurring in neural systems in general.

The mathematical models that take into account the delay effects in the nervous system are delay-differential equations (DDEs). These can be viewed as a kind of infinite dimensional version of the ordinary ones, and, consequently, the corresponding dynamical behaviour can be much more complex in the presence of delays. In spite of the fact that there can be found detailed mathematical analyses of delayed second-order differential equations (see Schurer 1948), the mechanical theory of balancing is well understood (see Roberts 1995), the central role of the time delay is recognized and analysed by neuropsychology (see Nijhawan 2008), the dynamics of a few interconnected neurons are analysed mathematically (see Campbell 2007) and the anatomy of the sensory systems are well described in biology (see Alcamo & Bergdahl 2003), there are only a few efforts that try to integrate this knowledge.

The goal of this paper is to connect the distant disciplines all related to the study of balancing, while the different aspects of balancing considered here are all the possible simplest ones. First, the low-degree-of-freedom (DoF) mechanical models are summarized that all lead to the same simple mathematical form, a second-order scalar DDE. Regarding the control part of balancing, the classical force/torque and stiffness control models are compared with those of the so-called velocity controls in non-holonomic systems and anticipatory ones, equivalencies and essential differences are pointed out. Then, the mathematical analysis of the underlying scalar DDE is presented, and the critical control parameters—including the time delays—are calculated in a simple way. With the help of all these results, the functioning of the sensory systems is summarized then from the view point of compensating for their own time delays. The ultimate goal is to understand and explain how our brain copes with these destabilizing delay effects in our nervous system.

2. Low-degree-of-freedom mechanical models of balancing

The simplest possible mechanical models are considered which can still characterize the most important dynamic effects of time delays. Although the task of balancing a body in gravitational space is usually a spatial problem, these models typically describe balancing in a single vertical plane only. The most popular mechanical models are derived and reviewed here.

(*a*) *Balancing on a horizontal straight bar*

Consider, for example, the task shown in figure 1*a*. In case we have to stand on a horizontal bar or a tensed rope, we can easily balance ourselves in the vertical plane spanned by the bar and our body, since the two feet placed along the bar

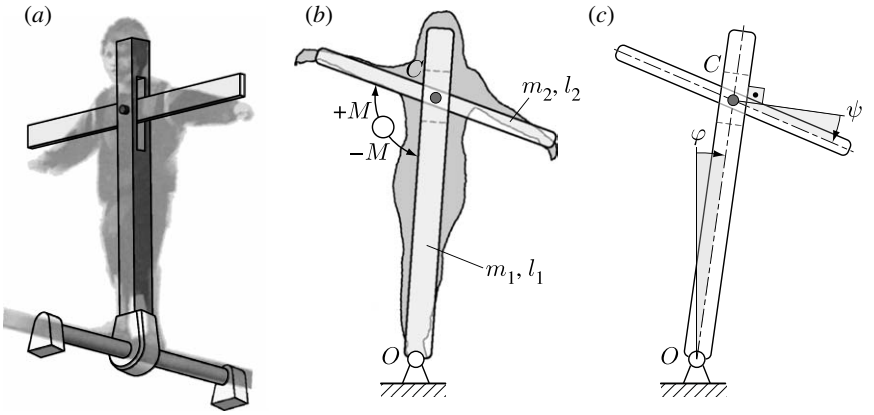

Figure 1. (*a*) Balancing on a straight bar. (*b*) The arms are used to stabilize the vertical position with the help of internal torques M applied between the arms and the body. (*c*) The corresponding mechanical model has two DoF with general coordinate φ of the body and ψ for the variation of the angle between the arms and the body.

provide two actuating forces in this sagittal plane partly supporting our weight and partly producing the necessary control torque vector normal to this plane (see the so-called stiffness control by Winter *et al.* (1998) later). However, our feet practically do not provide any torque about the bar, i.e. any torque vector having a line of action parallel to the bar. This means that it is rather difficult to balance ourselves in the vertical plane normal to the bar that we are walking on.

In these cases, there are two simple options to stand still and balance ourselves. One is that we use our arms as shown in figure 1*a* and rotate them about an axis parallel to the bar. Our arms are usually rotated in the same direction, with more or less the same orientation angle. The other option is to use the hip joint and bend our body in the plane normal to the bar. This option is used when we already have serious problems with standing on the bar. We are going to model the first, and actually simpler, behaviour.

The corresponding simplified mechanical model in the critical vertical plane is shown in figure 1*b*. The feet are substituted by a simple ideal joint at the point O, the vertical bar modelling the body has mass m_1 and mass moment of inertia J_{1O} with respect to the axis normal to the plane of the figure through O. The two arms are approximated to be aligned so they are substituted by a single bar having the total mass m_2 and mass moment of inertia J_{2C} with respect to the normal line via the centre of gravity of the arms denoted by C. We also use the notation $l = \overline{OC}$ for the distance of the joints O and C while l_1 and l_2 denote the height of the body and the span of the arms, respectively, where the corresponding centres of gravity are supposed to be at $l_1/2$ for the body, and at $l_2/2$, i.e. at the joint C, for the arms. If the body and the arms are modelled with these bars, for example, then $J_{1O} = m_1 l_1^2/3$ and $J_{2C} = m_2 l_2^2/12$.

The system has two DoF. The chosen general coordinates shown in figure 1*c* are $q_1 = \varphi$ and $q_2 = \psi$ where φ stands for the inclination of the bar $\overline{OC}$ representing the body, and ψ represents the variation of the angle between the line of the arms and the body. This angle normally varies about $\pi/2$. The two bars are connected by an ideal joint at C. Consequently, the $\varphi \equiv 0$ position is an equilibrium for any value of ψ.

Without control, this position is unstable, of course. The simplest way to stabilize it is to apply an internal torque M between the two bars about the normal axis through C. Actually, there are two torques here equal in magnitude and opposite to each other while acting on the two bars, but they have a non-zero power (and work), of course. Via the calculation of this power

$$-M\dot{\varphi} + M(\dot{\varphi} + \dot{\psi}) = \sum_{j=1}^{2} Q_j \dot{q}_j, \tag{2.1}$$

one obtains the general forces $Q_1 = 0$ and $Q_2 = M$. The Lagrangian equations then assume the form

$$\begin{pmatrix} J_{1O} + J_{2C} + m_2 l^2 & J_{2C} \\ J_{2C} & J_{2C} \end{pmatrix} \begin{pmatrix} \ddot{\varphi} \\ \ddot{\psi} \end{pmatrix} + \begin{pmatrix} -\left(\frac{1}{2} m_1 l_1 + m_2 l\right) g \sin \varphi \\ 0 \end{pmatrix} = \begin{pmatrix} 0 \\ M(\varphi, \dot{\varphi}) \end{pmatrix}. \tag{2.2}$$

If this internal torque M is chosen as the resultant of a virtual active spring and damper, i.e. a locally linear proportional-derivative (PD) controller is used in the form

$$M(\varphi, \dot{\varphi}) = P\varphi + D\dot{\varphi} + \text{h.o.t.}, \tag{2.3}$$

with h.o.t. representing the higher order terms of the angle φ and the angular velocity $\dot{\varphi}$, then the upper position can be stabilized with the appropriate choice of the scalar proportional and differential gains P and D.

Following the terminology of rational mechanics in Griffiths (1985) or Rand (1994), the second general coordinate ψ takes the role of a cyclic coordinate and the coupled equations of motion (2.2) can trivially be separated into two scalar differential equations; one for the essential coordinate φ in the form

$$(J_{1O} + m_2 l^2)\ddot{\varphi} - \left(\frac{1}{2} m_1 l_1 + m_2 l\right) g \sin \varphi = -M(\varphi, \dot{\varphi}), \tag{2.4}$$

which can be solved independently from ψ, and the other for the so-called hidden motion, which can be integrated directly from

$$\ddot{\psi} = \frac{M(\varphi, \dot{\varphi})}{J_{2C}} - \ddot{\varphi}. \tag{2.5}$$

The zero point of the hidden motion can be anywhere, although we consider $\psi = 0$ at the position where the arms and the body are normal to each other. It is likely that the normal position gives the most convenient way to apply this control. Before we analyse the mathematical model derived in (2.4) and (2.3), some further basic mechanical models of balancing are reviewed.

(*b*) *Balancing a stick and balancing ourselves in the sagittal plane*

While we presented the derivation of the mathematical models of balancing on a straight bar in detail, other mechanical models are briefly summarized only in this subsection. Figure 2*a* presents stick balancing on a fingertip or on a stretched open palm. This stick balancing could be a rough model for balancing

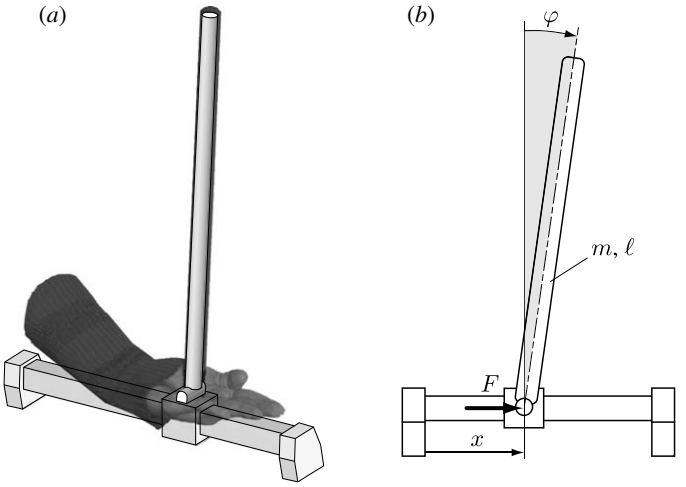

Figure 2. (*a*) Two-DoF mechanical model of stick balancing. (*b*) The general coordinates are the angle φ of the stick and the position x of its lowest point where there is an ideal joint. The control force F is horizontal.

our body in the sagittal plane when we use small steps to and fro to balance ourselves while our arms are not supposed to be in use. This is what we do when we try to stand still on the tips of skates on a paved surface.

The corresponding mechanical model of stick balancing has two DoF again and the convenient general coordinates are $q_1=\varphi$ and $q_2=x$ as shown in figure 2*b*. The control is established via the horizontal actuating force F at the slider, which gives the general forces $Q_1=0$ and $Q_2=F$. Note that the control force F is clearly external in the case of stick balancing. In the case of balancing ourselves on the tips of skates, this control force F is provided by the friction force that is controlled by us in an intricate way of walking strategies based on small internal torques at the hip and ankle joints (for more details see Coleman & Ruina (1998) and Piiroinen & Dankowicz (2005)). If the mass of the slider is negligible relative to the mass m of the bar of length l, the Lagrangian equations assume the form

$$\begin{pmatrix} \frac{1}{3}ml^2 & \frac{1}{2}ml\cos\varphi \\ \frac{1}{2}ml\cos\varphi & m \end{pmatrix} \begin{pmatrix} \ddot{\varphi} \\ \ddot{x} \end{pmatrix} + \begin{pmatrix} -\frac{1}{2}mgl\sin\varphi \\ -\frac{1}{2}ml\dot{\varphi}^2\sin\varphi \end{pmatrix} = \begin{pmatrix} 0 \\ F(\varphi,\dot{\varphi}) \end{pmatrix}. \quad (2.6)$$

This time, x takes the role of the 'cyclic' coordinate that can be eliminated to be left with a scalar second-order differential equation for the essential coordinate φ

$$\frac{1}{12}(4-3\cos^2\varphi)ml^2\ddot{\varphi} + \frac{1}{8}ml^2\dot{\varphi}^2\sin(2\varphi) - \frac{1}{2}mgl\sin\varphi = -\frac{1}{2}F(\varphi,\dot{\varphi})l\cos\varphi, \quad (2.7)$$

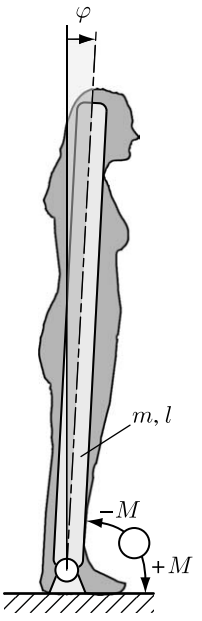

Figure 3. One-DoF mechanical model of balancing ourselves in the sagittal plane. The ankle joint provides the necessary control torque M between our feet and legs.

which is used with the same PD-like control

$$F(\varphi, \dot{\varphi}) = P\varphi + D\dot{\varphi} + \text{h.o.t.}, \tag{2.8}$$

as in (2.3) the units of P and D are different, however.

Finally, figure 3 shows a one-DoF model of balancing ourselves in the sagittal plane via the torques applied at the ankle joint that is called stiffness control (Winter *et al.* 1998) in neurophysiology. For the single general coordinate $q_1 = \varphi$, the Lagrangian equation and the attached control torque assume the form

$$\frac{1}{3} ml^2 \ddot{\varphi} - \frac{1}{2} mgl \sin \varphi = -M(\varphi, \dot{\varphi}), \tag{2.9}$$

$$M(\varphi, \dot{\varphi}) = P\varphi + D\dot{\varphi} + \text{h.o.t.}, \tag{2.10}$$

respectively. At this point, we briefly review other possible ways of modelling these simple PD control strategies on the introductory example of balancing on a straight bar.

(*c*) *Non-holonomic constraints versus anticipatory systems*

Instead of the control torque M in (2.3), it is a natural idea to try to model the control of the system in figure 1*c* as a constraint established between the essential coordinate φ and the cyclic coordinate ψ. Clearly, a simple geometric constraint between ψ and φ as $\psi = P\varphi + \text{h.o.t.}$ cannot be established since there are no corresponding constraining forces, i.e. there are no actuators available which could determine the inclination φ of the body relative to the vertical direction defined by the gravitational acceleration vector. The same applies for the application of a possible linear non-holonomic constraint

$$\dot{\psi} = P\varphi + D\dot{\varphi}, \tag{2.11}$$

where the corresponding Lagrangian equations extended by the Lagrange multiplier Λ would assume the form

$$\begin{pmatrix} J_{1O} + J_{2C} + m_2 l^2 & J_{2C} \\ J_{2C} & J_{2C} \end{pmatrix} \begin{pmatrix} \ddot{\varphi} \\ \ddot{\psi} \end{pmatrix} + \begin{pmatrix} -\left(\frac{1}{2} m_1 l_1 + m_2 l\right) g \sin \varphi \\ 0 \end{pmatrix} = \begin{pmatrix} -D\Lambda \\ \Lambda \end{pmatrix} \tag{2.12}$$

and the coupled algebraic differential equations (2.12) and (2.11) determine the magnitude of the constraining torque, which is exactly Λ (see Griffiths 1985). Clearly, there is no actuator that could provide the torque $(-D\Lambda)$ with respect to the angle φ of the body—only the other constraining torque Λ is available via the internal actuation between the body and the arms.

All these observations mean that the classical methods of rational mechanics should not be applied here in a standard way; in spite of the fact that controlling the velocities of DC actuators is a widely used strategy in robotics, they can rarely be modelled as non-holonomic constraints. The way these strategies could easily be modelled is given in the theory of anticipatory systems, where the 'constraint' (2.11) provides a kind of prediction for the relative angular velocity $\dot{\psi}$ based on just the previous values of the sensed angle φ and angular velocity $\dot{\varphi}$. If the constrained angular velocity $\dot{\psi}$ is realized with a simple PD-like control as in (2.11), however, the control torque M is not the result of a direct PD control any more; it is determined in a more complicated way by the substitution of the derivative of equation (2.11) of the form

$$\ddot{\psi} = P\dot{\varphi} + D\ddot{\varphi}, \tag{2.13}$$

into the second equation of (2.2); that is, we obtain this control torque as a function $M(\varphi, \dot{\varphi}, \ddot{\varphi})$. In the meantime, substitution of (2.13) into the first equation of (2.2) results in

$$\left(J_{1O} + J_{2C}(1 + D) + m_2 l^2\right)\ddot{\varphi} + J_{2C} P\dot{\varphi} - \left(\frac{1}{2} m_1 l_1 + m_2 l\right) g \sin \varphi = 0, \tag{2.14}$$

which clearly shows that this kind of PD control cannot stabilize the upward position, as no control term appears there to compensate the negative stiffness originated in the gravitational force acting on the inverted pendulum.

This lengthy train of thought leads to the observation that the velocity control of the actuating electric motors preferred in robotics should work as a proportion-integral control as

$$\dot{\psi} = P\varphi + I \int_0^t \varphi(\vartheta) \mathrm{d}\vartheta, \tag{2.15}$$

with proportional gain P and integral gain I. From the view point of stability and qualitative dynamical behaviour, this leads to a control strategy that is equivalent to the PD-like torque control introduced in (2.3) above. Since the derivative of (2.15) yields

$$\ddot{\psi} = P\dot{\varphi} + I\varphi, \tag{2.16}$$

where P takes the role of the differential gain and I takes the role of the proportional gain in (2.3), the substitution of (2.16) into the first equation of (2.2) results in

$$(J_{1O} + m_2 l^2)\ddot{\varphi} + J_{2C}P\dot{\varphi} + J_{2C}I\varphi - \left(\frac{1}{2}m_1 l_1 + m_2 l\right) g \sin\varphi = 0, \tag{2.17}$$

which is practically equivalent to the system formed by (2.4) and (2.3). Consequently, without loss of generality, we can discuss only the PD-like control for the internal torque as introduced in (2.3), and only the case (2.4) of balancing on a straight bar is analysed in the rest of this study.

Still, we have to keep in mind another important observation in the theory of anticipatory systems: the control action—either M in (2.3) or $\ddot{\psi}$ in (2.16)—has to be predicted because it cannot be taken at the same time instant as the observation of the signals φ and $\dot{\varphi}$. In the case of digital control in robotics, the minimum value of this delay is the sampling time in the system, which could be in the range of milliseconds in practice; but in the case of human balancing, this delay is rather in the range of hundreds of milliseconds to even one second (see Nijhawan 2008).

3. Stability in the presence of time delay

Consider the task of balancing on a straight bar and its equation of motion (2.4) for the essential coordinate φ, and introduce a constant time delay τ in the control (2.3) to obtain the extended mathematical description

$$M(\varphi_t, \dot{\varphi}_t) = P\varphi(t-\tau) + D\dot{\varphi}(t-\tau) + \text{h.o.t.}, \tag{3.1}$$

where the subscript t in the symbolic expression on the left-hand side refers to the functions of the state variables with respect to the past instead of their actual values. It is expressed with a single explicit delayed value in its actual form on the right-hand side. Then the nonlinear equation of motion of balancing on a straight bar (figure 1) is constructed from (2.4) and (3.1)

$$\begin{aligned}(J_{1O} + m_2 l^2)\ddot{\varphi}(t) - \left(\frac{1}{2}m_1 l_1 + m_2 l\right) g \sin\varphi(t) \\ = -P\varphi(t-\tau) - D\dot{\varphi}(t-\tau) + \text{h.o.t.},\end{aligned} \tag{3.2}$$

which is a DDE having an infinite dimensional phase space (for an introduction, see Hale & Lunel (1993)).

The consideration of a single deterministic time delay both at the angle and at the angular velocity signals in (3.2) is a rough approximation since the delay must also depend on the actual combinations of the sensory systems in use and on the ways they are actually functioning. Still, there are several measurement data described by Nijhawan (2008) which support this approach, although many different clusters of neurons are involved in the process parallel to each other.

(*a*) *Stability of the upward position*

The trivial solution $\varphi \equiv 0$ of the nonlinear DDE (3.2) represents the upward position of the inverted pendulum in figure 1*c*. The stability of this upward position is investigated with the help of the variational system of (3.2), which is the result of linearization at $\varphi \equiv 0$

$$(J_{1O} + m_2 l^2)\ddot{\varphi}(t) + D\dot{\varphi}(t-\tau) + P\varphi(t-\tau) - \left(\frac{1}{2} m_1 l_1 + m_2 l\right) g\varphi(t) = 0. \quad (3.3)$$

Introduce the new notation for the gains p and d, and the angular natural frequency ω_{n} of the uncontrolled system having small oscillations at the downward position about $\varphi = \pi$

$$p = \frac{P}{J_{1O} + m_2 l^2}, \quad d = \frac{D}{J_{1O} + m_2 l^2}, \quad \omega_{\mathrm{n}} = \sqrt{\frac{\left(\frac{1}{2} m_1 l_1 + m_2 l\right) g}{J_{1O} + m_2 l^2}}, \quad T = \frac{2\pi}{\omega_{\mathrm{n}}}, \quad (3.4)$$

where the corresponding time period of small oscillations is denoted by T. Then the simplified form of the variational system assumes the form

$$\ddot{\varphi}(t) + d\dot{\varphi}(t-\tau) + p\varphi(t-\tau) - \omega_{\mathrm{n}}^2 \varphi(t) = 0. \quad (3.5)$$

It is easy to see that the linearized form of equations (2.7) and (2.8) of stick balancing, or those of equations (2.9) and (2.10) of the stiffness control in the sagittal plane, or even the linearized form of equation (2.17) of the anticipatory-like model of balancing on a straight bar, have the same mathematical form as (3.5) with different kinds of definitions for the parameters p, d and ω_{n}. This means that the analysis of the linear DDE (3.5) has a central role in the theory of balancing.

Early stability analyses of DDEs such as (3.5) appeared in the 1940s (see Minorsky 1942; Schurer 1948; or Hayes 1950) before the basic mathematical theory of DDEs was established as an infinite dimensional system by Myshkis (1949). Since then, many examples have been studied that require detailed linear analysis and the corresponding nonlinear investigation of second-order delayed systems (e.g. Campbell *et al.* 1995; Stepan & Kollar 2000; Niculescu 2001; Landry *et al.* 2005). All these results construct the characteristic function of (3.5) via the substitution of the exponential trial solution $A\exp(\lambda t)$, $A,\ \lambda \in C$ (or by Laplace transformation)

$$\lambda^2 + d\lambda \mathrm{e}^{-\tau\lambda} + p\mathrm{e}^{-\tau\lambda} - \omega_{\mathrm{n}}^2 = 0. \quad (3.6)$$

The trivial solution is (exponentially) asymptotically stable in the Lyapunov sense if and only if all the infinitely many characteristic roots of the characteristic equation (3.6) have negative real parts. Stability criteria, such as the ones of Stepan (1989) and Sipahi & Olgac (2006), can be used to carry out this test. Clearly, there exists a pure imaginary characteristic root $\lambda = \mathrm{i}\omega$, $\omega \in [0, \infty)$ at the limit of asymptotic stability. Substitute this root into (3.6) and separate the real and imaginary parts of the resulting complex equation

$$-\omega^2 + d\omega \sin(\omega\tau) + p\cos(\omega\tau) - \omega_{\mathrm{n}}^2 = 0, \quad d\omega\cos(\omega\tau) - p\sin(\omega\tau) = 0. \quad (3.7)$$

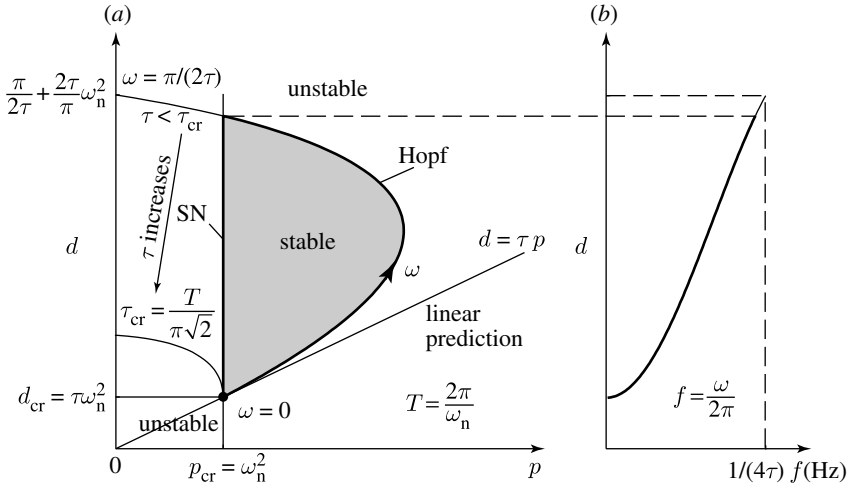

Figure 4. (*a*) The shaded stability region in the parameter plane of the proportional gain p and differential gain d. The stable domain disappears for delay parameters larger than the critical τ_{cr}. The linear prediction line touches the stable region at the critical values of the gains. (*b*) The vibration frequencies of the self-excited vibration occurring at the Hopf limit of stability are shown.

This technique is also called the D-subdivision method by Kolmanovskii & Nosov (1986). The stability boundaries in the parameter space are among these ω-parametrized surfaces. If the system parameter ω_n and the delay parameter τ are fixed, the equations (3.7) can be reformulated

$$\left.\begin{aligned} \text{for } \omega=0: \quad & p=\omega_n^2, \quad d\in(-\infty,+\infty),\\ \text{for } \omega>0: \quad & p(\omega)=\left(\omega^2+\omega_n^2\right)\cos(\omega\tau),\\ & d(\omega)=\left(\omega^2+\omega_n^2\right)\frac{\sin(\omega\tau)}{\omega}. \end{aligned}\right\} \tag{3.8}$$

These are ω-parametrized curves in the parameter plane (p, d) shown in figure 4*a*. With the help of the lengthy implicit differentiation of the characteristic function with respect to the gain parameters p and d in (3.6), one can show that a real characteristic root crosses the imaginary axis of the complex plane from left to right when the proportional gain p is decreased through the boundary defined for $\omega=0$ in (3.8), while a complex pair of characteristic roots crosses the imaginary axis from left to right each time when the spiralling curve in (3.8) is crossed with the gain parameters from inside to outside, i.e. with increasing values of (p^2+d^2) radially in the (p, d) plane.

The above calculations result in the stability chart presented in figure 4*a*. The shaded stability region in the (p, d) parameter plane has a straight line boundary for $\omega=0$ in (3.8) where saddle-node (SN) or pitchfork bifurcation may occur in the original nonlinear system (2.4) and (2.3), while Hopf bifurcation may lead to self-excited vibrations at the boundary in (3.8) for $\omega\in(0,\pi/(2\tau))$ and $p>\omega_n^2$. The frequency $f=\omega/(2\pi)$ of these self-excited vibrations varies in the range

$$f\in\left(0,\frac{1}{4\tau}\right), \tag{3.9}$$

given in the units Hz as shown in figure 4*b*. These vibration frequencies arise typically when too large gains are used in the presence of relatively large time delays, which is in the parameter region located to the right of the shaded domain of stability in figure 4.

(*b*) *Critical delay and critical gain parameters of linear predictions*

It is easy to check that the stability region shrinks with increasing values of the delay parameter τ. Moreover, the stable region disappears and the balancing of the inverted pendulum is impossible with any linear PD controller if

$$\tau > \tau_{\mathrm{cr}}. \tag{3.10}$$

In order to determine the critical value τ_{cr} of the delay parameter, consider the critical gain parameter point

$$\left.\begin{aligned} p_{\mathrm{cr}} &= \omega_{\mathrm{n}}^2 \;\Rightarrow P_{\mathrm{cr}} = \left(\frac{1}{2} m_1 l_1 + m_2 l\right) g, \\ d_{\mathrm{cr}} &= \tau \omega_{\mathrm{n}}^2 \Rightarrow D_{\mathrm{cr}} = \tau P_{\mathrm{cr}}. \end{aligned}\right\} \tag{3.11}$$

At these parameters, the simplest possible anticipation strategy is applied: the proportional gain is set just at the minimal necessary value to achieve stability without time delay, and the differential gain is set in a way that the actual orientation angle φ is predicted by estimating the motion with a uniform rotation of constant angular velocity, and the control torque is selected to be proportional to this predicted value $\tilde{\varphi}$ of the angle

$$M(\varphi_t, \dot{\varphi}_t) = P_{\mathrm{cr}}\varphi(t) + D_{\mathrm{cr}}\dot{\varphi}(t) = P_{\mathrm{cr}}(\varphi(t-\tau) + \tau\dot{\varphi}(t-\tau)) = P_{\mathrm{cr}}\tilde{\varphi}(t). \tag{3.12}$$

The behaviour of a tennis player returning a fast tennis ball was explained in the same way by Nijhawan (2008). At this point, the simplest linear prediction with the finite-difference method coincides with the PD control providing the necessary virtual spring stiffness and virtual viscous damping to stabilize an otherwise unstable system in accordance with the Newtonian laws.

Expand the Taylor series of $p(\omega)$ in (3.8) about $\omega = 0$

$$p(\omega) = \omega_{\mathrm{n}}^2 + \left(1 - \frac{1}{2}\tau^2\omega_{\mathrm{n}}^2\right)\omega^2 + - \cdots. \tag{3.13}$$

Locally, at the critical gain parameter point (3.11), the proportional gain parameter starts increasing with increasing ω if the coefficient of ω^2 is positive; that is, the stable region exists if and only if

$$\tau < \tau_{\mathrm{cr}} = \frac{\sqrt{2}}{\omega_{\mathrm{n}}} = \frac{T}{\pi\sqrt{2}}. \tag{3.14}$$

This means that the maximal time delay τ_{cr} allowed in the case of successful balancing can be determined by measuring the time period T of small oscillations of the same mechanical structure hanging at its stable (downward) position, then calculating by (3.14).

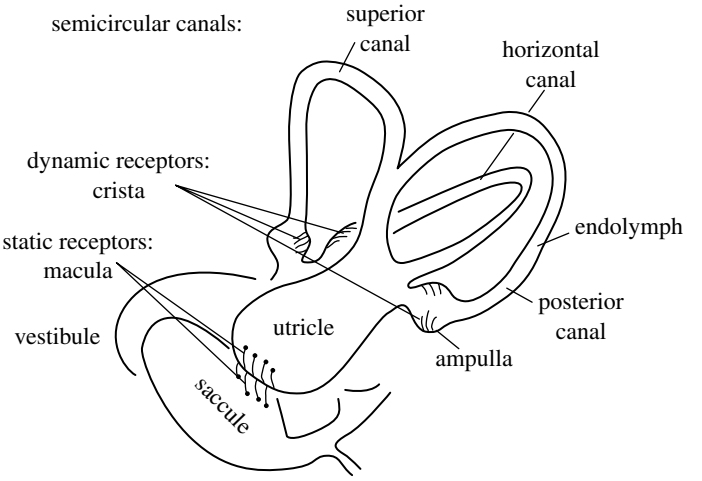

Figure 5. Labyrinth—the balancing organ. Its static and dynamic receptors provide the necessary angle and angular velocity signals to balance the body in the presence of time delays in the auditory neural pathways.

The zoo of the different kinds of dynamic behaviour around the critical parameter point (3.11) was described thoroughly by Sieber & Krauskopf (2004) via the exploration of the intricate multiple degenerate bifurcation there.

4. Sensory systems compensating for their own delay

Many sensory systems support us during balancing. They all have to provide both angle and angular velocity signals since the domain of stability in figure 4 is essentially separated from the axes of the gain parameters, the upward position is unstable if either the proportional gain P or the differential gain D is zero. Among these sensory systems, first, we mention the one that provides signals about the pressure distribution between the ground and the feet supporting the body, then the balancing organ in the inner ear called the labyrinth, and finally the most important faculty and its organ, the eye. The functioning of the pressure sensors in our feet (see Winter *et al.* 1998) and their relationship to improved balancing due to slight stochastic perturbations are discussed by Moss & Milton (2003). In what follows, the labyrinth and the eye are analysed from the viewpoint of coping with time delays in the Newtonian mechanics to ensure successful balancing.

(*a*) *The labyrinth and the auditory subsystem of balancing*

A schematic view of the balancing organ, called the labyrinth, is shown in figure 5. The balancing organ is located in the inner ear (see Alcamo & Bergdahl 2003) and it has two important units often referred to as static and dynamic receptors; one is responsible for providing signals about the inclination of our head and the other is responsible for providing signals about angular velocity components of the head. This is in perfect accordance with the result of the analysis of the Newtonian equations with delay: both angle and angular velocity signals are needed during balancing (see the stability chart in figure 4).

Look at the static receptor, first. As shown in figure 5, the so-called vestibule contains two chambers, the utricle and the saccule. There are two sensitive parts of the skin there: the macula at the bottom of the utricle and the macula at the top of the saccule. They provide the angle signal in an intricate way, since this sensor has no perfect information about the absolute vertical direction defined by the gravitational acceleration. At this point, more sophisticated mechanical models are to be developed in order to explain how the static receptor part of the labyrinth works.

As shown in figure 5, the crista provides the angular velocity signal. This hairy part covered with a gelatinous dividing partition called the cupula is located in the ampulla (figure 5). The three ampullae are situated at the stems of the three semicircular canals lying in three planes normal to each other. The liquid called endolymph in the corresponding semicircular canal moves relative to the duct wall and provides a signal in the crista owing to the viscous damping between the endolymph and the cupula.

This system seems to work as a perfect velocity sensor. However, the endolymph is not at rest as the head is rotating in the same direction for longer periods of time: it accelerates owing to the viscous friction between the duct wall and the liquid and starts rotating together with the head. Consequently, the viscous damping force decreases and the brain starts missing the angular velocity signal in this situation. Moreover, when we stop suddenly after a long period of rotation, the endolymph moves forward and gives the false sensation of rotating in the opposite direction via opposite excitation of the crista. Clearly, the mechanical model used in the case of balancing on a straight bar (see figure 1 and (3.2)) is weak in this respect, since it assumes that the angular velocity $\dot{\varphi}$ is known perfectly after a certain time delay—consequently, this model cannot describe the above-explained 'dizziness'. If we improve this model by introducing two further general coordinates, namely the deformation of the hair in the crista and the angle of the endolymph in the canal, the mechanical system will have four DoF, and analysis of the much more complex equations shows that balancing is still possible in the presence of time delay, too. This analysis can be found in Stepan & Kollar (2000), where the model of an artificial labyrinth is also discussed in detail.

People without any liquid in their inner ear suffer from so-called 'dry ear'. In this case, the angular velocity signal is not provided by the labyrinth, for certain. Balancing is impossible in these cases if no other sensory system can help, for example when our feet are aligned on a bar and no pressure signal is provided and our eyes are also closed. In the subsequent section, we check how the visual system works from the viewpoint of balancing.

(*b*) *The eye and the visual subsystem of balancing*

Generally speaking, the visual system seems to be much more reliable than the auditory one in the sense that it can detect the head's inclination relative to the vertical direction quite well using the images of walls, trees or any other well-known vertically positioned objects. However, we must keep in mind that the neural delay along the visual pathway in the brain is much larger than those of the auditory pathways, which are still slower than the mechanoreceptors of the touch system (see details in Nijhawan 2008). This is not necessarily related to the physical lengths of the pathways, but also (or rather) to the time needed for the additional cortical processing of the signals.

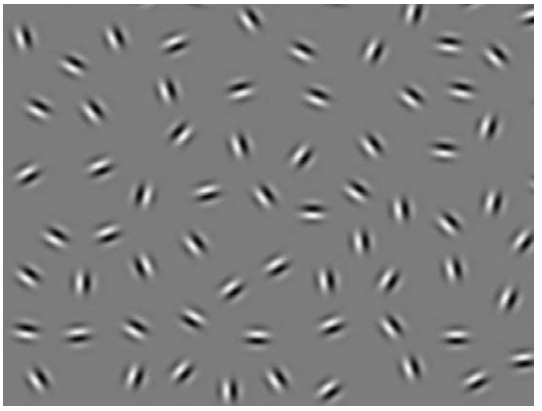

Figure 6. Gabor elements representing the orientation-defined contour stimulus. The stimulated path is a circle in the centre of the picture. Adapted with permission from Kovacs (2000).

It has been known for a long time (see Wertheimer 1938) that the so-called 'law of good continuation' helps to recognize a number of geometric illusions as an object or just as a certain path of elements in visual perception (see Field *et al.* 1993). The so-called Gabor signals roughly model the receptive field properties of orientation selective simple cells in the primary visual cortex; therefore, they are appropriate stimuli for the examination of these small spatial filters and their interactions (see the circular path in figure 6, taken from Kovacs (2000)). The reason why these tiny elements with different orientation angles are used in psychological experiments has a physiological background.

Light stimulates the photoreceptors in the eye and the detected tiny different orientation signals are mapped through the visual neural pathway onto the surface of the visual cortex in the brain (see Nicholas & Swindale 1996). The different colours in figure 7*a* show the different stimulus orientations that best activate the corresponding coloured regions of the cortex. This way our brain is able to recognize geometrical objects such as circles (see the one in figure 6), and it is 'easy' to recognize straight lines characterized by their orientations; we especially need to identify the vertical ones in order to determine the inclination of our body during balancing (see angle φ in figure 1*c*).

In the meantime, we must keep in mind that balancing does not work with the angle signal only when time delays are present (see the stability chart in figure 4). If the brain tried to produce the velocity signal by using additional cortical processing, then the time delay would be increased so much that balancing would be impossible in the same way as the tennis player would not be able to return a fast ball (see the analysis in Nijhawan 2008).

The enlarged region of the visual cortex in figure 7*b* shows the corresponding colour-coded orientation preference, and the arrows in the regions also denote the so-called direction preference. This means, for example, that the green region sensitive to vertical orientation tends to be stimulated by horizontal velocity (see Weliky *et al.* 1995 or Sincich & Blasdel 2001). Consequently, the most important part of a complex image we see during balancing is not only the inclination of a vertical straight line relative to our body; our visual system also detects its angular velocity. A hypothetical model of Nijhawan (2008) also provides

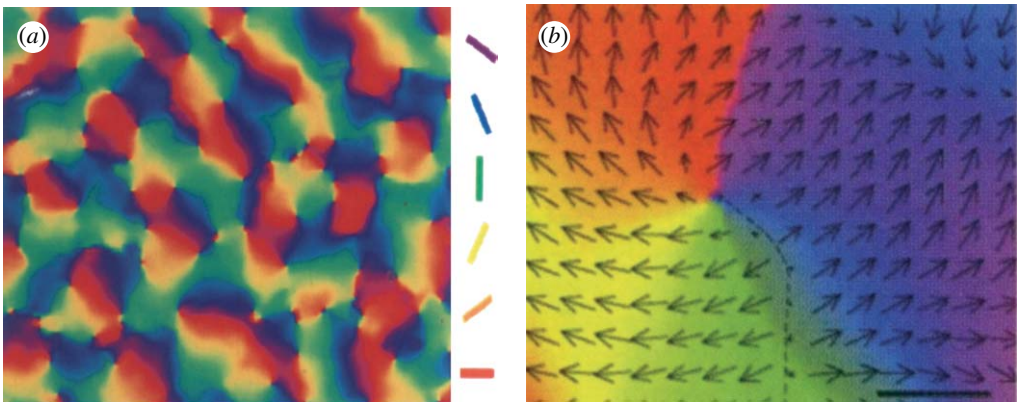

Figure 7. (*a*) Coloured regions of the visual cortex sensitive to the corresponding orientation-defined stimuli. The colour code is defined by the orientations in the middle section. The data were obtained by optical recording from the visual cortex of a macaque monkey. Adapted with permission from Blasdel (1992). (*b*) The enlarged section of the coloured visual cortex also represents the direction preference denoted by arrows roughly normal to the orientation preferences. Adapted with permission from Weliky *et al.* (1996).

a possible explanation of how the horizontal and vertical neural pathways might actually produce velocity signals with a kind of finite-difference method realized physically among the cells, and how it might predict the image 'ahead' through layers of excitatory and inhibitory interactions in the retina.

5. Concluding remarks

The mathematical analysis of the basic mechanical models of balancing in the presence of time delays together with the observations related to the functioning of the auditory system including the balancing organ, the labyrinth, and the vision system including the eyes gives a specific view of the functioning of our brain. These systems have to cope with their own neural delays, i.e. in the centre of the mechanical task, which is actually the stabilization of a multiple inverted pendulum.

Many one- and two-DoF mechanical models of balancing can be simplified to second-order scalar DDEs having a standard linearized form (3.5) at the upward position of the pendulum. The stability analysis of this equation results in the stability chart in figure 4. The most important conclusions related to this chart are as follows.

Simple PD control can be used for balancing in the presence of time delay, but increasing time delays tend to destabilize dynamical systems. Although this statement does not always apply for second-order systems (see Stepan 1989), the rule of thumb is valid for balancing with delay. The larger the delay is, the more difficult it is to find appropriate PD control gains to stabilize the system. For delays exceeding a critical value, the system is always unstable. This maximal delay belonging to successful balancing can be determined by measuring the time period of small oscillations of the same mechanical structure hanging as a non-inverted

pendulum at its stable (downward) position, and this time period has to be divided then by the irrational numbers π and $\sqrt{2}$ (see (3.14)). Clearly, the larger the mass moment of inertia of the mechanical system is, the larger the time period of oscillation is, and consequently the balancing task is easier to carry out. For the simple case of stick balancing (figure 2), this means that the longer the stick is, the easier it is to balance it. The practical limit is at a stick of 0.3 m in length where the critical time delay is approximately 0.1 s, which is a common value from the eyes to the arm. Shorter sticks, such as pencils, can be balanced by reducing the delay further, for example by placing the pencil on a knife held in our mouth.

Another conclusion provided by the stability chart of figure 4 is that both the angle and the angular velocity signals are needed to accomplish the task successfully with a simple PD controller. In case the velocity signal is missing from the sensory system, the brain would need much more time to establish a more complex control strategy based on two or even more past values of the position signals. This would increase the time delay substantially, and that costs stability (see Changizi 2008). This might be one of the reasons why our auditory and visual systems provide both position and velocity signals at the same time in a very efficient and fast way. That is how these sensory systems help to compensate for the neural delay mainly caused by themselves.

It is also worth mentioning that the linear prediction based on an estimated uniform motion does not guarantee balancing. If the actual position is predicted by summing up the past position and the past velocity multiplied by the delay, then the corresponding P, D gains might be close to but still below the region of stability shown in figure 4.

Along the stability limit for maximal proportional gain P, self-excited vibrations arise with frequencies varying from 0 to $1/(4\tau)$. These low-frequency oscillations in the range of 1 Hz are observed when tipsy people try to walk, or when we have to stand with our eyes closed and our feet aligned.

There are still many open questions. Some of these are related to the problems of sensing absolute angles relative to vertical direction or absolute angular velocities, also discussed briefly related to the labyrinth sketched in figure 5. Another question is how the brain copes with balancing a stick of 0.3 m when the time delay must be in the range of 0.1 s, while the visual system works much more 'slowly' if the signals are sent up to the appropriate regions of the visual cortex. A 'short' neural pathway through the so-called medial temporal loop of the brain might be one of many possible explanations.

The study of the Newtonian equations of balancing will certainly provide further conclusions for the study of the brain itself via the central role of time delays in the dynamics of balancing. However, it is not only classical mechanics that could be applied in research in neurophysiology and neuropsychology. If we are going to explain the small amplitude stochastic oscillations that are observed even in those cases when balancing is considered to be practically stable and successful, we can apply the results in the field of chaotic dynamics of nonlinear mechanical systems such as the ones in Haller & Stepan (1995) or Enikov & Stepan (1998). The description of micro-chaotic motions in digitally controlled unstable systems could serve as an alternative explanation as to why the finite sensitivity of the auditory and/or the visual system leads to the small-amplitude stochastic oscillations of the body while standing still. This stochastic oscillation is also discussed by Yao *et al.* (2001) or by Milton *et al.* (2009) with the help of

stochastic DDEs. As explained by Moss & Milton (2003), enhancing these oscillations may improve balancing abilities of elderly people, which is one of the many possible applications of the results in medical technology.

This research was partially supported by the Hungarian Scientific Research Foundation OTKA under grant no. K68910. The author is grateful for inspiring discussions on neuropsychological aspects with Ilona Kovacs. The author would also like to thank Jan Sieber for drawing his attention to the early paper of Schurer (1948).

References

Alcamo, E. & Bergdahl, J. 2003 *Anatomy coloring workbook*. Princeton, NJ: The Princeton Review.

Blasdel, G. G. 1992 Orientation selectivity, preference, and continuity in monkey striate cortex. *J. Neurosci.* **12**, 3139–3161.

Campbell, S. A. 2007 Time delays in neural systems. In *Handbook of brain connectivity* (eds A. R. McIntosh & V. K. Jirsa). New York, NY: Springer Verlag.

Campbell, S. A., Belair, J., Ohira, T. & Milton, J. 1995 Limit cycles, tori, and complex dynamics in a second-order differential equation with delayed negative feedback. *J. Dyn. Differ. Equ.* **7**, 213–236. (doi:10.1007/BF02218819)

Changizi, M. A. 2008 The trade-off between speed and complexity. *Behav. Brain Sci.* **31**, 203. (doi:10.1017/S0140525X08003853)

Coleman, M. & Ruina, A. 1998 An uncontrolled toy that can walk but cannot stand still (Tinkertoy Walker). *Phys. Rev. Lett.* **80**, 3658–3661. (doi:10.1103/PhysRevLett.80.3658)

Enikov, E. & Stepan, G. 1998 Micro-chaotic motion of digitally controlled machines. *J. Vib. Control* **4**, 427–443. (doi:10.1177/107754639800400405)

Field, D. J., Hayes, A. & Hess, R. F. 1993 Contour integration by the human visual system: evidence for a local 'association field'. *Vision Res.* **33**, 173–193. (doi:10.1016/0042-6989(93)90156-Q)

Griffiths, J. B. 1985 *The theory of classical dynamics*. Cambridge, UK: Cambridge University Press.

Hale, J. K. & Lunel, S. M. V. 1993 *Introduction to functional differential equations*. New York, NY: Springer Verlag.

Haller, G. & Stepan, G. 1995 Micro-chaos in digital control. *J. Nonlin. Sci.* **6**, 415–448. (doi:10.1007/BF02440161)

Hayes, N. D. 1950 Roots of the transcendental equation associated with a certain differential-difference equation. *J. Lond. Math. Soc.* **25**, 226–232. (doi:10.1112/jlms/s1-25.3.226)

Kolmanovskii, V. B. & Nosov, V. R. 1986 *Stability of functional differential equations*. London, UK: Academic Press.

Kovacs, I. 2000 Human development of perceptual organization. *Vision Res.* **40**, 1301–1310. (doi:10.1016/S0042-6989(00)00055-9)

Landry, M., Campbell, S. A., Morris, K. & Aquilar, C. O. 2005 Dynamics of an inverted pendulum with delayed feedback control. *SIAM J. Appl. Dyn. Syst.* **4**, 333–351. (doi:10.1137/030600461)

Milton, J., Townsend, J. L., King, M. A. & Ohira, T. 2009 Balancing with positive feedback: the case for discontinuous control. *Phil. Trans. R. Soc. A* **367**, 1181–1193. (doi:10.1098/rsta.2008.0257)

Minorsky, N. 1942 Self-excited oscillations in dynamical systems possessing retarded actions. *ASME J. Appl. Mech.* **9**, 65–72.

Moss, F. & Milton, J. G. 2003 Medical technology—balancing the unbalanced. *Nature* **425**, 911–912. (doi:10.1038/425911a)

Myshkis, A. D. 1949 General theory of differential equations with delay. *Uspekhi Matematicheskikh Nauk* **4**, 99–141. [Engl. Transl. 1951 *AMS* **55**, 162].

Nicholas, V. & Swindale, N. V. 1996 Visual cortex: looking into a Klein bottle. *Curr. Biol.* **6**, 776–779. (doi:10.1016/S0960-9822(02)00592-4)

Niculescu, S.-I. 2001 *Delay effects on stability: a robust control approach*. New York, NY: Springer Verlag.

Nijhawan, R. 2008 Visual prediction: psychophysics and neurophysiology of compensation for time delays. *Behav. Brain Sci.* **31**, 179–198. (doi:10.1017/S0140525x08003804)

Piiroinen, P. T. & Dankowicz, H. J. 2005 Low-cost control of repetitive gait in passive bipedal walkers. *Int. J. Bifurcat. Chaos* **15**, 1959–1973. (doi:10.1142/S0218127405013083)

Rand, R. H. 1994 *Topics in nonlinear dynamics*. Amsterdam, The Netherlands: Gordon & Breach.

Roberts, T. D. M. 1995 *Understanding balance: the mechanics of posture and locomotion*. London, UK: Chapman & Hall.

Schurer, F. 1948 Zur Theorie des Balancierens. *Mathematische Nachrichten* **1**, 295–331. (doi:10.1002/mana.19480010506)

Sieber, J. & Krauskopf, B. 2004 Bifurcation analysis of an inverted pendulum with delayed feedback control near a triple-zero eigenvalue. *Nonlinearity* **17**, 85–104. (doi:10.1088/0951-7715/17/1/006)

Sincich, L. C. & Blasdel, G. G. 2001 Oriented axon projections in primary visual cortex of the monkey. *J. Neurosci.* **21**, 4416–4426.

Sipahi, R. & Olgac, N. 2006 Stability robustness of retarded LTI systems with single delay and exhaustive determinations of their imaginary spectra. *SIAM J. Control Optim.* **45**, 1680–1696. (doi:10.1137/050633238)

Stepan, G. 1989 *Retarded dynamical systems*. London, UK: Longman.

Stepan, G. & Kollar, L. 2000 Balancing with reflex delay. *Math. Comput. Model.* **31**, 199–205. (doi:10.1016/S0895-7177(00)00039-X)

Weliky, M., Kandler, K., Fitzpatrick, D. & Katz, L. C. 1995 Patterns of excitation and inhibition evoked by horizontal connections in visual cortex share a common relationship to orientation columns. *Neuron* **15**, 541–552. (doi:10.1016/0896-6273(95)90143-4)

Weliky, M., Bosking, W. H. & Fitzpatrick, D. 1996 A systematic map of direction preference in primary visual cortex. *Nature* **379**, 725–728. (doi:10.1038/379725a0)

Wertheimer, M. 1938 *Laws of organization in perceptual forms*. London, UK: Harcourt (Brace & Jovanovich).

Winter, D. A., Patla, A. E., Prince, F., Ishac, M. & Gielo-Perczak, K. 1998 Stiffness control of balance in quiet standing. *J. Neurophys.* **80**, 1211–1221.

Yao, W., Yu, P. & Essex, C. 2001 Delayed stochastic differential model for quiet standing. *Phys. Rev. E* **63**, 021902. (doi:10.1103/PhysRevE.63.021902)